Technical Report

TR-02-08

Numerical modelling of fracture displacements due to thermal load from a KBS-3 repository

Hakami Eva, Olofsson Stig-Olof

Itasca Geomekanik AB

January 2002

Svensk Kärnbränslehantering AB
Swedish Nuclear Fuel
and Waste Management Co
Box 5864
SE-102 40 Stockholm Sweden
Tel 08-459 84 00
+46 8 459 84 00
Fax 08-661 57 19
+46 8 661 57 19

Numerical modelling of fracture displacements due to thermal load from a KBS-3 repository

Hakami Eva, Olofsson Stig-Olof

Itasca Geomekanik AB

January 2002

Keywords: Thermo-mechanical effects, thermal load, fracture, displacement, shear strength, fracture size, fracture dip, fracture stiffness, numerical modelling, UDEC, FLAC^{3D}

Abstract

The objective of the project has been to estimate the largest shear displacements that could be expected on a pre-existing fracture located in the repository area, due to the heat release from the deposited waste.

Two-dimensional numerical analyses using the "Universal Distinct Element Code" (UDEC) have been performed. The UDEC models represent a vertical cross section of a KBS-3 type repository with a large planar fracture intersecting a deposition hole at the repository centre. The extension, dip and mechanical properties of the fracture were changed in different models to evaluate the influence of these parameters on fracture shear displacements. The fracture was modelled using a Coulomb slip criterion with no cohesion and no dilation. The rock mass surrounding the fracture was modelled as a homogeneous, isotropic and elastic material, with a Young's modulus of 40 GPa. The initial heat release per unit repository area was assumed to be 8W/m² (total power/total repository area).

The shear displacements occur due to the thermal expansion of the rock surrounding the heat generating canisters. The rock mass is almost free to expand vertically, but is constrained horizontally, which gives a temperature-induced addition of shear stresses in the plane of the fracture. The shear movement of the fracture therefore follows the temperature development in the surrounding rock and the maximum shear displacement develops about 200 years after the waste deposition.

Altogether, twenty cases are analysed. The maximum shear displacement, which occurs at the fracture centre, amounts to 0.2–13.8 cm depending on the fracture parameters. Among the analysed cases, the largest shear values, about 13 cm, was calculated for the cases with about 700 m long fractures with a shear stiffness of 0.005 GPa/m. Also, for large fractures with a higher shear stiffness of 5 GPa/m, but with a low friction angle (15°), the shear displacement reaches similar magnitudes, about 10 cm. A fracture of 265 m length, 30° dip angle, 5 GPa/m shear stiffness and 30° friction angle gave 4.5 cm shear displacement.

In the two-dimensional UDEC models, the fracture extension is defined as the length L along the dip direction of the fracture. In reality, however, the three-dimensional geometry of the fracture will influence the shear magnitude. Results from additional three-dimensional analyses (using FLAC^{3D}) offer a comparison between two cases regarding the three-dimensional extension of a fracture. A model assuming a fracture with infinite extension in the strike direction, and a length L in the dip direction, i.e. the 2-D assumption made in the UDEC analyses, gives 1.4 times larger fracture shear displacement than a corresponding model with a circular fracture of diameter L.

Among the different parameters varied between models in this study, the fracture friction length, fracture friction angle and shear stiffness are found to be the most important for the heat induced shear displacement on the fracture plane.

With regard to the current safety limit for allowed fracture shear displacements (10 cm), the following approximate layout restriction i suggested: Central parts of fractures dipping in the range of 30°– 45° with a minimum length of 700 metres in the dip direction, and a friction angle smaller than about 15° or shear stiffness in the order of 0.005 GPa/m or less, should not be allowed to intersect the deposition holes. This recommendation is only valid for the over all conditions assumed in this study. A significantly different initial stress state or change in thermal loading could lead to a different layout criterion.

Sammanfattning

Syftet med projektet har varit att uppskatta den största skjuvrörelse som kan förväntas ske längs en spricka som korsar förvarsområdet, på grund av termisk belastning från det deponerade avfallet.

Tvådimensionella numeriska analyser med hjälp av ”Universal Distinct Element Code” (UDEC) har utförts. UDEC-modellen representerar en vertikalsektion genom förvaret där ett tänkt sprickplan korsar ett depositionshål i förvarets mitt. Utbredningen, stupningen och de mekaniska egenskaperna hos sprickan varierades mellan modellerna för att undersöka dessa parametrars betydelse för beräknad skjuvrörelse i sprickplanet. Sprickan simulerades med Coulombs kriterium utan kohesion och utan dilatation. Bergmassan som omgav sprickan simulerades som ett homogent, isotropt och elastiskt material med 40 GPa elastiticitetsmodul. Den initiella värmeeffekten har i analysen antagits motsvara 8 W/m² (total effekt/total förvarsyta).

På grund av den termiska expansion som induceras i berget omkring de värmegenererande kapslarna erhålls skjuvdeformationer. Bergmassan har möjlighet att expandera i det närmaste fritt i vertikalled men är inspänd i horisontalled. Detta leder till en temperaturinducerad ökning av skjuvspänningen i sprickplanet. Sprickans skjuvrörelse följer därför temperaturutvecklingen i omgivande berg och den största skjuvdeformationen fås ca 200 år efter deponering.

Sammanlagt 20 modeller analyserades. Resultaten visar att den största skjuvdeformationen, vid sprickans mitt, uppgår till 0,2–13,8 cm i de tjugo modellerna, beroende på sprickparametrarna. De största skjuvrörelserna, omkring 13 cm, beräknades för fallen med cirka 700 m långa sprickor med 0.005 GPa/m skjuvstyvhet. Även för långa sprickor med en högre skjuvstyvhet (5 GPa/m), men med låg friktionsvinkel (15°), blir skjuvdeformationen av samma storleksordning, cirka 10 cm. En 265 m spricka med 30° friktionsvinkel och 30° stupning resulterade i 4.5 cm maximal skjuvdeformation.

Sprickans utbredning är i de två-dimensionella UDEC-beräkningarna definierad som längden, L, i stupningsriktningen. Men i verkligheten har sprickans tredimensionella utbredning betydelse för skjuvdeformationens storlek. Resultat från kompletterande tredimensionella analyser (med hjälp av ha FLAC^{3D}) gör det möjligt att jämföra två fall när det gäller en enskild sprickas tre-dimensionella utbredning. Den modell som simulerar en spricka med oändligt lång utsträckning i strykningsriktningen, med längden L i stupningsriktning (dvs samma antaganden som i den tvådimensionella UDEC-modellen), ger 1,4 gånger större maximal skjuvdeformation jämfört med en cirkulär spricka med diametern L.

Sprickplanets utbredning, friktionsvinkel och skjuvstyvhet är de parametrar som visat sig ha störst betydelse för skjuvdeformationen, bland de parametrar som varierats mellan modellerna i denna studie.

Med hänsyn till gällande säkerhetsgräns för tillåten skjuvning av sprickor (10 cm), föreslås följande approximativa layout-kriterium: Centrala delar av sprickor som stupar 30°–45°, som är minst 700 meter långa i stupningsriktningen och har en friktionsvinkel lägre än 15° eller en skjuvstyvhet på 0.005 GPa/m eller mindre, ska inte tillåtas skära depositionshålen. Denna rekommendation är endast giltigt för de generella förhållanden som antagits i denna studie. Ett signifikant förändrat initiellt spänningstillstånd eller termisk belastning skulle kunna leda till ett annat layoutkriterium.

Contents

1 Introduction

1.1 Background

The primary function of a deep repository for spent nuclear fuel is to *isolate* the waste. If this isolation should be breached, the deep repository is also supposed to *retard* the transport of radionuclides from the fuel. The canister, the buffer and the host rock work in conjunction to provide these two functions.

Concerning the requirements on the host rock, the SKB RD&D-Program 98 /SKB, 1998/ states that to fulfil the isolating and retarding function the bedrock must:

> *"– constitute a mechanically stable environment for the deep repository,*
>
> *– provide a chemical environment that is long-term stable and favourable with respect to the function of the other barriers,*
>
> *– minimise the risk of future intrusions and alternative uses (e.g. mines)"*

This study relates to the first of these requirements, i.e. the mechanical stability of the rock around the repository. One of the concerns in this respect is the possibility of a large displacement occurring on a pre-existing fracture intersecting a deposition hole. Such a large displacement might jeopardise the intactness of a waste canister, i.e. break the isolation. A large fracture displacement might also result in increased ground water transport from the deposition hole to the surrounding rock mass, i.e. reduce the retardation.

The concern about a large fracture shear displacement is therefore one of the items in the assessment of the long-term safety, SR 97, carried out by SKB. The SR 97 Background Report /SKB, 1999/ states:

> *"The most fundamental mechanical process in the geosphere from the safety viewpoint is movements in large discontinuities."*

The same report further presents how the shear displacements of pre-existing fractures currently are handled in the safety assessment:

> *"Criteria can be set up for direct shear movements across deposition holes. At present, the criterion is that shear movements exceeding 0.1 m should be avoided to prevent canister damages. There are no equivalent general criteria for permeability changes."*

One of the aims of the SKB studies is hence to be able to show that the fracture shear displacement criteria will be met. This can be achieved by gaining good confidence concerning the possible span for parameters describing the load situation, the rock and the fracture properties at the repository site. With this prerequisite, numerical modelling is a tool to predict fracture displacements that may be expected under different conditions, and numerically computed estimates of movements may be compared with existing criteria.

A multi-phase investigation with the objective to investigate the global thermo-mechanical aspects of storing spent nuclear fuel in a KBS-3 type repository was carried out during 1995–1997 /Hakami et al. 1998/. This investigation mainly focused on large scale effects, i.e. on thermomechanically induced changes in stresses and fracture zone displacements at a large distance from the repository itself. The study involved a three-dimensional simulation of a site with bedrock similar to Äspö. Several large sub-vertical fracture zones intersected the rock mass block surrounding the hypothetical heat generating waste repository. The size of the fracture zones was large, 4,000x4,000 m, but with fixed boundaries. The friction angle adopted was 20°. The results showed a maximum fracture zone shear displacement of about 3 cm. It should be noted, however, that the fracture zones in this study were oriented more or less parallel to the principal stress directions and that no inclined or sub-horizontal fracture zone were simulated. This means that the zones simulated had a favourable orientation, not giving the largest possible displacement. However, the results clearly illustrated how thermally induced stresses are affected by the choice of repository layout as well as on the geological conditions at a future site.

The main difficulty in estimating the movements of large rock discontinuities, such as fracture zones or even minor faults, is the lack of knowledge concerning their mechanical properties /Leijon, 1995/. For the purpose of safety analyses it thus makes it inevitable to choose parameter values within wide ranges. If it is assumed that a discontinuity can be approximated as a singular planar structure where the shear displacement is mainly controlled by friction, the most conservative case is a zero friction angle. Results from an analytical calculation of a two-dimensional case with a frictionless fracture are presented in the Background Report to SR 97, see Figure 3-1 based on /Pollard and Segall, 1987/. These calculations indicate that, with the most unfavourable orientation, the size of a discontinuity should be on the order of 100 m to get a displacement of 0.1 m.

The intention with the analyses performed in this study was to add to the current state of knowledge by performing numerical analyses of a two-dimensional case, in principle similar to that in Figure 1-1, but with assumptions somewhat closer to the real repository situation. The thermal load due to the temperature development from the canisters has been calculated and the corresponding mechanical response with time determined in a thermo-mechanically coupled model has been evaluated.

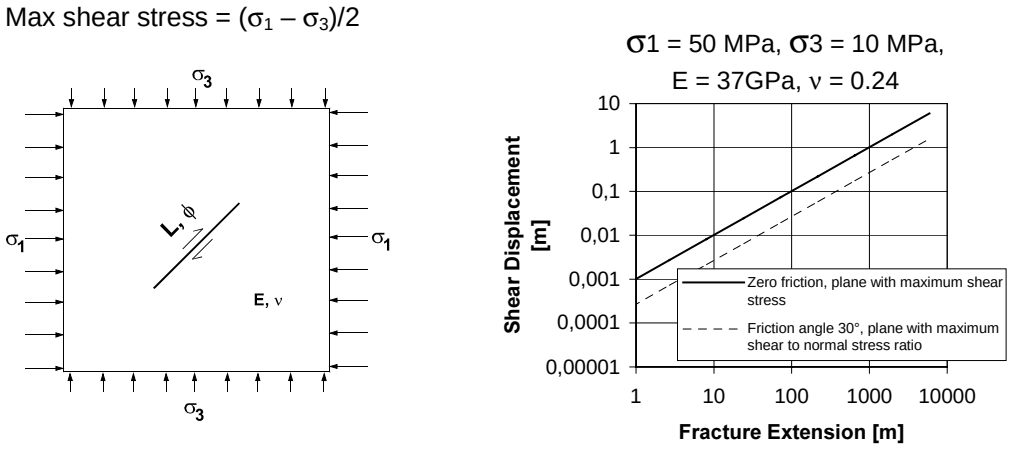

Figure 1-1. *Fracture with extension L, and friction angle ϕ in elastic medium with the elastic parameters E and ν. The shear deformation is maximum at the centre of the fracture and zero at the edges.*

1.2 Objectives

The objective of the project has been to estimate the largest shear displacements that could be expected on a pre-existing fracture located in the repository area, due to thermal loading from the deposited waste. The displacement should be estimated for fractures of different extensions and orientations. The importance of fracture shear strength properties should also be evaluated.

The estimated shear displacement was to be compared with the current canister damage criterion regarding fracture shear displacements across deposition holes. According to this criterion, shear displacements of 0.1 m or more count as canister damages.

1.3 Scope of study

The actual geometry of a future repository site will be complex and truly three-dimensional. Nevertheless, for this generic study, the approach to the problem has been to simplify the problem by looking at only one single, continuous and planar fracture. This simplification can be regarded as conservative, since in reality it can be expected that the thermally induced shear stresses would be released by deformations along many fractures , resulting in less shear deformation on each individual fracture. The fracture is also assumed to have the most disadvantageous location, i.e. with the central part intersecting the repository horizon, and conservative assumptions are made concerning the fracture properties. Two-dimensional analyses using UDEC /Itasca, 2000/ have been performed. UDEC is a distinct element code with the ability to explicitly represent discontinuities.

The fracture is given the most disadvantageous orientation with respect to the in-situ stress field, i.e. a strike perpendicular to the largest horizontal stress, and with respect to the repository openings, i.e. a strike parallel to the tunnels. Different models with

different fracture dip angles and extensions are analysed. The in-situ stress magnitudes are chosen as being representative of typical Swedish bedrock and are the same in all models.

The behaviour of the discontinuity will, apart from its extension, location and orientation, be dependent on the mechanical properties of the solid rock and the fractures. Mechanical properties of rock discontinuities (faults, joints) vary within wide ranges. For this study the fracture is simulated with a Coulomb slip behaviour with no cohesion and no dilation. The friction angle has been given different values in different models. The influence of different fracture stiffness parameters has also been evaluated.

One restriction to the model is that it does not account for fracture propagation, i.e. the extension of a pre-defined fracture is fixed.

2 Numerical model

2.1 Model geometry

The UDEC model represents a vertical cross section of the repository and has a width of 1400 m and a height of 900 m, see Figure 2-1. The waste repository is assumed to have 25 TBM tunnels with 40 metres spacing. The fracture (or fault) under study intersects a deposition hole in the central part of the repository.

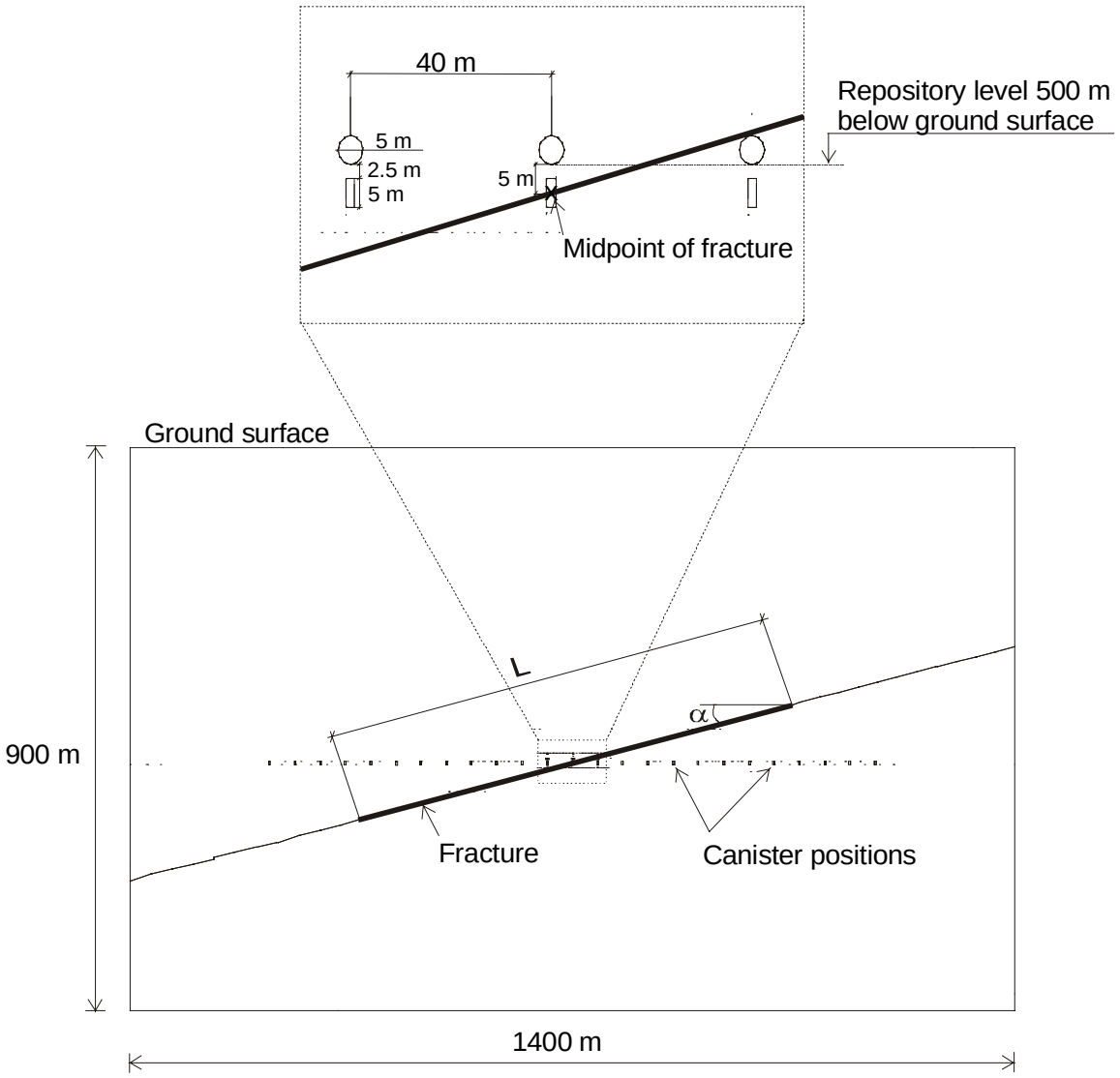

Figure 2-1. *UDEC model geometry. In the Figure, the fracture length, L, is 719 m and the fracture dip, α, is 15°.*

The stress re-distribution caused by excavation of tunnels at some distance from the fracture does not contribute significantly to the fracture displacements. Therefore, only the three central tunnels were modelled explicitly and excavated in a separate step in the modelling sequence. Beneath each tunnel position a block was created to represent the heat generating canisters. In the modelling work, different fracture extensions and orientations were analysed. A summary of the different fracture geometries is given in Figure 2-2. The exact fracture length is determined by the zoning in each model, which in turn depends on the dip angle.

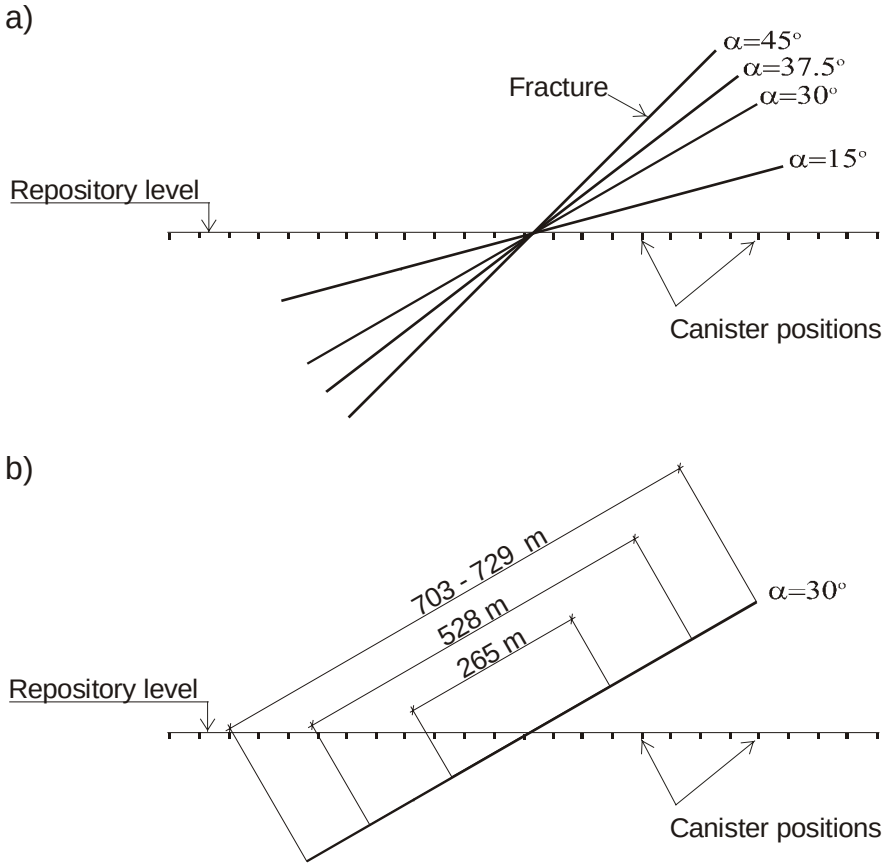

Figure 2-2. *Summary of fracture geometries a) dip angles used in the study and b) fracture lengths.*

2.2 Mechanical model

The rock mass surrounding the fracture was modelled as a homogeneous, isotropic and elastic material, with a Young's modulus of 40 GPa and a Poisson's ratio of 0.22.

The fracture was modelled with a Coulomb slip criterion and the fracture parameters used are given in Table 2-1. These parameters were altered between different models to evaluate their influence on fracture shear displacements. The fracture was simulated with no cohesion and no dilation. Apart from the fracture of interest in this study, artificial fractures (or joints) were used to define tunnel boundaries, canister positions and zoning regions. For the artificial joints high stiffness and high strength parameters were used so that these joints would not influence the modelling result.

Table 2-1. Fracture property and geometric parameters used in the models.

Model	Dip angle, α [°]	Friction angle, ϕ [°]	Normal stiffn., Kn [GPa/m]	Shear stiffn., Ks [GPa/m]	Fracture length, L [m]
M1	15	15	10	5	719
M2	30	15	10	5	703
M3	45	15	10	5	729
M4	45	15	100	5	729
M5	30	15	10	5	528
M6	30	15	10	5	265
M7	30	30	10	5	703
M8	30	45	10	5	703
M9	37.5	15	10	5	706
M10	30	30	10	5	528
M11	30	30	10	5	265
M12	30	5	10	5	528
M13	45	15	100	50	729
M14	15	30	10	5	719
M15	45	30	10	5	729
M16	45	30	100	5	729
M17	45	15	10	0.005	729
M18	45	15	0.1	0.005	729
M19	30	15	0.1	0.005	703
M20	30	30	0.1	0.005	703

The in-situ stress state measured at Äspö was taken to be the initial stress condition in the model /Rehn et al., 1997/. The major horizontal stress was oriented perpendicularly to the repository tunnels. This orientation is the most unfavourable with respect to shear stress on the fracture intersecting the repository in the two-dimensional model. In the fracture, pore pressures were initiated corresponding to a ground water level situated at ground surface. The effective stresses in the fracture are then used to calculate fracture displacements. Initial total stresses, σ, in the rock mass and pore pressures, U, in the fracture were applied according to the equations below.

$$\sigma_H = 5.0 + 2\sigma_v \text{ [MPa]} \quad (2\text{-}1)$$

$$\sigma_v = \rho_r \cdot g \cdot z \cdot 10^{-6} \text{ [MPa] with } \rho_r = 2700 \text{ [kg/m}^3\text{]} \quad (2\text{-}2)$$

$$U_{Fracture} = \rho_w g \cdot z \cdot 10^{-6} \text{ [MPa] with } \rho_w = 1000 \text{ [kg/m}^3\text{]} \quad (2\text{-}3)$$

Where z is the depth in metres below the ground surface and g the gravitational acceleration (9.81 m/s^2).

The fracture is not mechanically stable, under the imposed initial stresses, for all variations in fracture friction angles and fracture geometry. The models were calculated to equilibrium and the equilibrated state represents the “in-situ” stress state (See also Section 3.1).

The mechanical boundary conditions for the model are zero normal displacement for the vertical boundaries and lower horizontal boundary. The upper horizontal boundary, representing the ground surface, was modelled as a free surface.

2.3 Thermal model

The thermal properties are assumed to be isotropic, homogenous and constant throughout the rock mass, and only heat transfer by conduction in the rock mass is modelled. This means that the presence of the fracture does not influence the calculated thermal field and that effects of heat convection by fluid flow or fluid buoyancy were neglected. The contribution from convection is very small and it is also conservative to neglect it. The thermo-mechanical calculations performed involve a one-way coupling, such that changes in the temperature field affect the stress field through the linear expansion coefficient, but that heat generated by friction, for example, was ignored. Since the movements are very slow the friction heat can be shown to be negligibly small. Thermal properties for the rock mass are given in Table 2-2.

Table 2-2. Thermal properties for the rock mass.

Property	Value
Specific heat [J/kg°C]	741
Thermal conductivity [W/m°C]	3.0
Linear expansion coefficient [1/°C]	8.5E–6

The heat release decay function applied in the model is defined by the following equation /Thunvik and Braester, 1991/:

$$Q(t)/Q_0 = \left(\alpha_1 e^{-\alpha_2 t} + (1-\alpha_1)e^{-\alpha_3 t}\right) \qquad (2\text{-}4)$$

Where *Q(t)* denotes the time-dependent heat release,
Q_0 denotes the heat release at the time of the deposition,
t is the time [years],
$\alpha_1 = 7.531212\text{x}10^{-1}$,
$\alpha_2 = 2.176060\text{x}10^{-2}$ [years^{-1}], and
$\alpha_3 = 1.277985\text{x}10^{-3}$ [years^{-1}].

A time period up to 1000 years after deposition was simulated. The initial heat release for each canister (Q_0), i.e. heat release at the time of waste deposition, is set to 1200 W With a canister spacing of 25 m by 6 m, the corresponding initial heat release per unit repository area will be 8.0 W/m^2. An initial heat release per meter tunnel was assigned to the canister blocks in the two-dimensional model. Since the thermal effects are only due to temperature increase, the initial temperature was set to zero in the entire model.

Adiabatic boundary conditions were used for the outer boundaries, e. i. no heat transfer occurs across these boundaries. These thermal boundary conditions give slightly overestimated temperatures. The interior of the tunnels was assumed to have the same thermal properties as the surrounding rock mass.

2.4 Modelling sequence

The modelling sequence consisted of three major stages:

1. Initiation of initial stresses and pore pressures in fracture. (Calculation to equilibrium).

2. Excavation of the three central tunnels in the repository. (Calculation to equilibrium).

3. Simultaneous emplacement of all waste canisters. Coupled thermo-mechanical calculations to a maximum time of 1,000 years after deposition.

The main model result after each stage will be presented in the following chapter. A total of twenty different models were analysed.

3 Results

3.1 In-situ conditions

The general stress pattern in the Swedish bedrock is an increasing horizontal and vertical stress with depth. However, due to the inhomogeneity in the rock mass the actual stress distribution may deviate from this pattern. In the case of a large single fracture of low strength it is plausible to expect the stress pattern to be affected by the presence of the fracture. In this modelling study the stress situation around the fracture was established by first initiating a regular depth-dependent stress field in the entire model, and thereafter calculate the equilibrium stress field, reached after slip along the fracture in some of the models. The stress state at equilibrium represents the in-situ stress state in this study.

The Mohr circle diagram in Figure 3-1 illustrates how the dip angle for the fracture in the model and the friction angle assumed for the fracture will determine whether slip occurs on the fracture due to the initiated stresses or not. The diagram gives the span of dip angles for which a fracture at 500 meters depth will slip, for the three different friction angles used in this study.

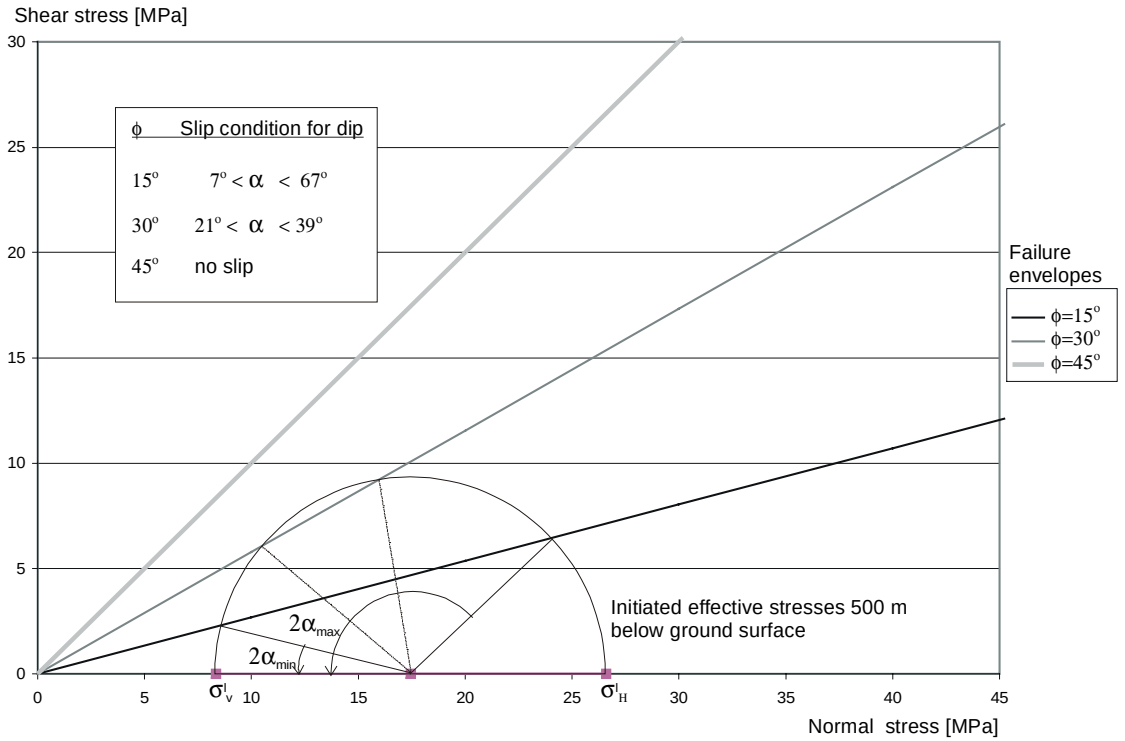

Figure 3-1 Mohr circle construction illustrating slip condition for different fracture friction angles, ϕ, and dip angles, α.

The result from the calculation of in-situ stress state for seven different cases are summarised in Figure 3-2. The maximum displacement necessary to reach equilibrium is given for different dip and friction angles. In this diagram all models have a fracture with a length of about 700 m. It can be noted that the numerical results are in agreement with the slip criterion presented in Figure 3-1. In two of the models the fracture is not at

slip for the in-situ stress condition. All displacements calculated in this stage are set to zero before the excavation of the tunnels. Displacements resulting from the excavation stage are set to zero prior to the thermal loading as well.

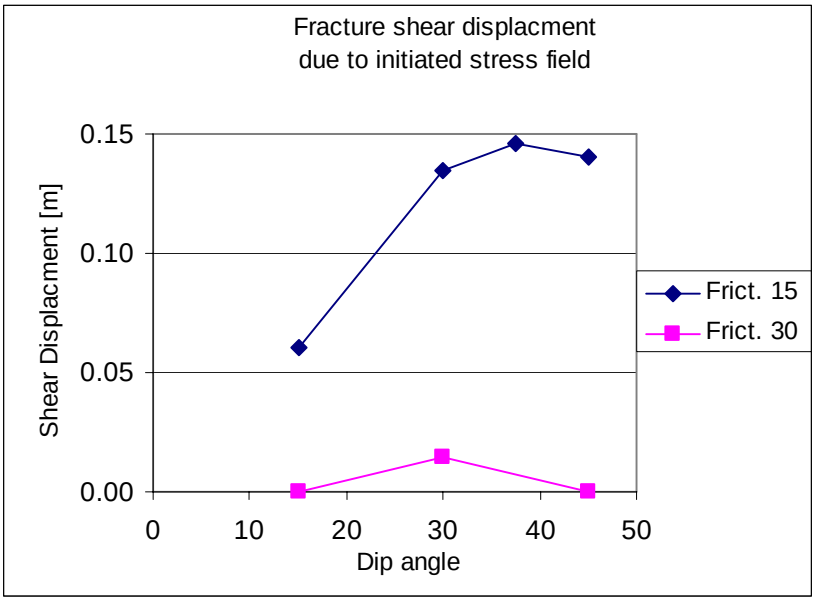

Figure 3-2. *Maximum fracture shear displacements in models due to initiated stresses. The maximum shear displacement occurs at the centre of the fracture.*

3.2 Excavation of repository tunnels

The excavation of the central three deposition tunnels gives an additional shear stress on the fracture. However, the contribution is fairly small and the shear displacement is ≤ 3 mm for model M1and ≤ 1.3 mm for model M14. The general pattern of calculated shear displacements for this modelling stage are similar for all models and only a few illustrating examples are therefore shown, see Figure 3-3.

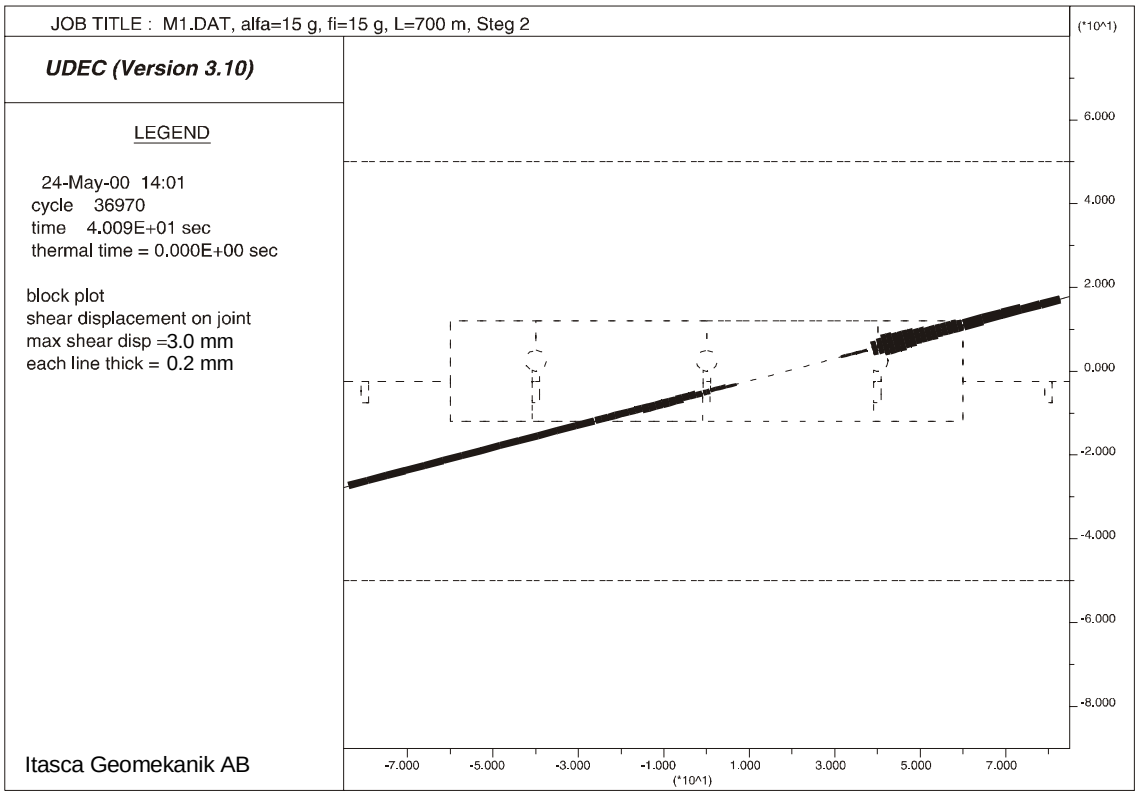

a)

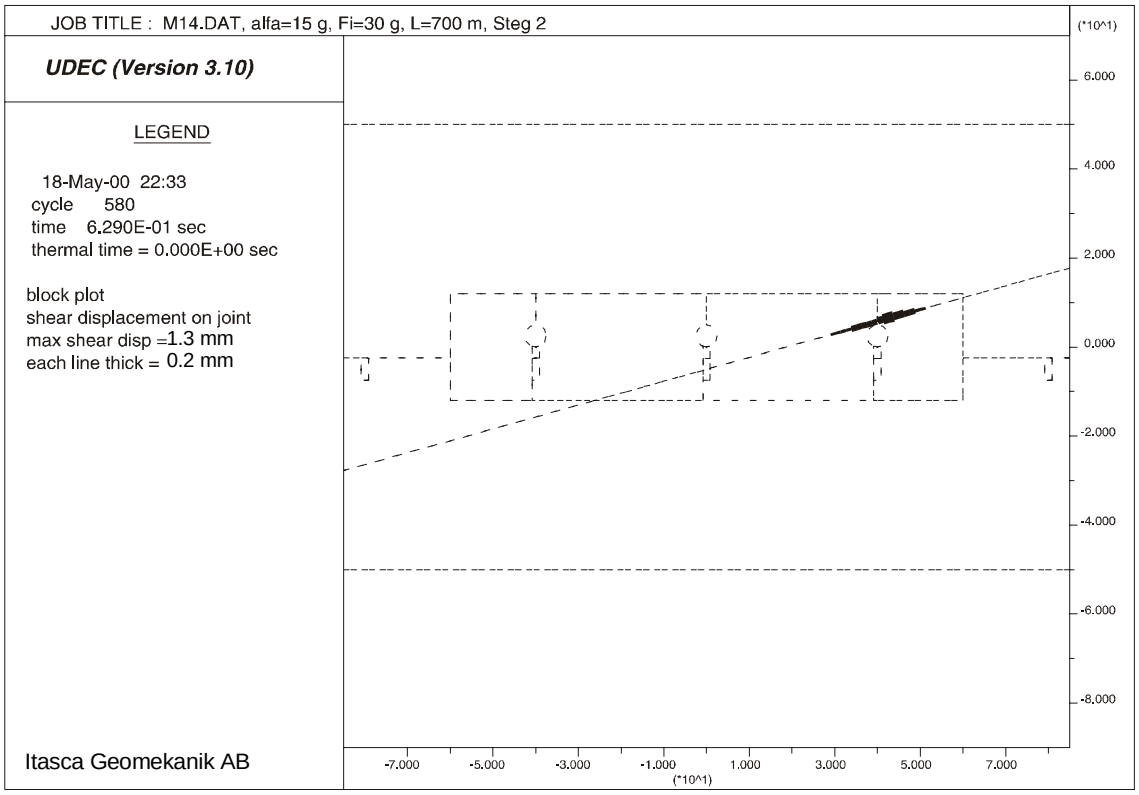

b)

Figure 3-3. *Shear displacements due to excavation for: a) Model M1(α=15°, ϕ=15° and L=719 m) and b) Model M14 (α=15°, ϕ=30° and L=703 m). The dashed lines are artificial joints that define tunnel boundaries, canister positions and different zoning regions.*

3.3 Thermal loading

3.3.1 Temperature development

The temperature distribution in the rock mass will develop identically in all models. As an example, the temperature distribution after 200 years is shown in Figure 3-4. The temperature development with time may be better understood by looking at Figure 3-5 which shows the temperature for three locations in the model (marked in Figure 3-4). Note that the temperatures given are the temperature increases. The actual temperature in the repository is determined by adding the initial ambient temperature. (Since the thermo-mechanical properties are all assumed to be temperature independent, thermo-mechanical effects are caused by temperature changes, not total temperatures).

Close to the repository the temperature will rise quickly. Between tunnels the maximum temperature is reached after 50 years . This temperature is almost constant up to 1000 years. (Beyond 1000 years the heat release decay function used is not applicable). At large distances from the repository the temperature will rise more slowly. This difference will also show up as differences in shear development with time between fractures with different angles, i.e. for fractures located at different distance from the repository (See Section 3.3.3).

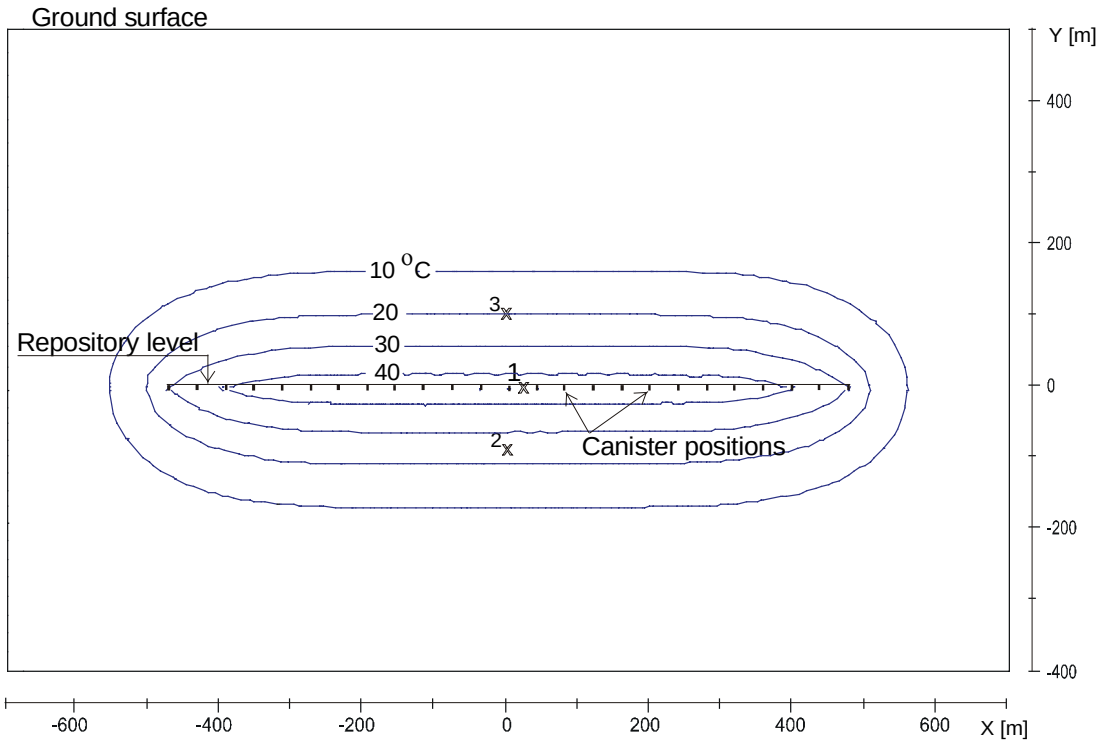

Figure 3-4. *Temperature increase after 200 years of deposition.(To get the expected total temperatures, the initial in-situ depth dependent temperatures must be added.) Three points where temperature development was recorded are marked in the figure.*

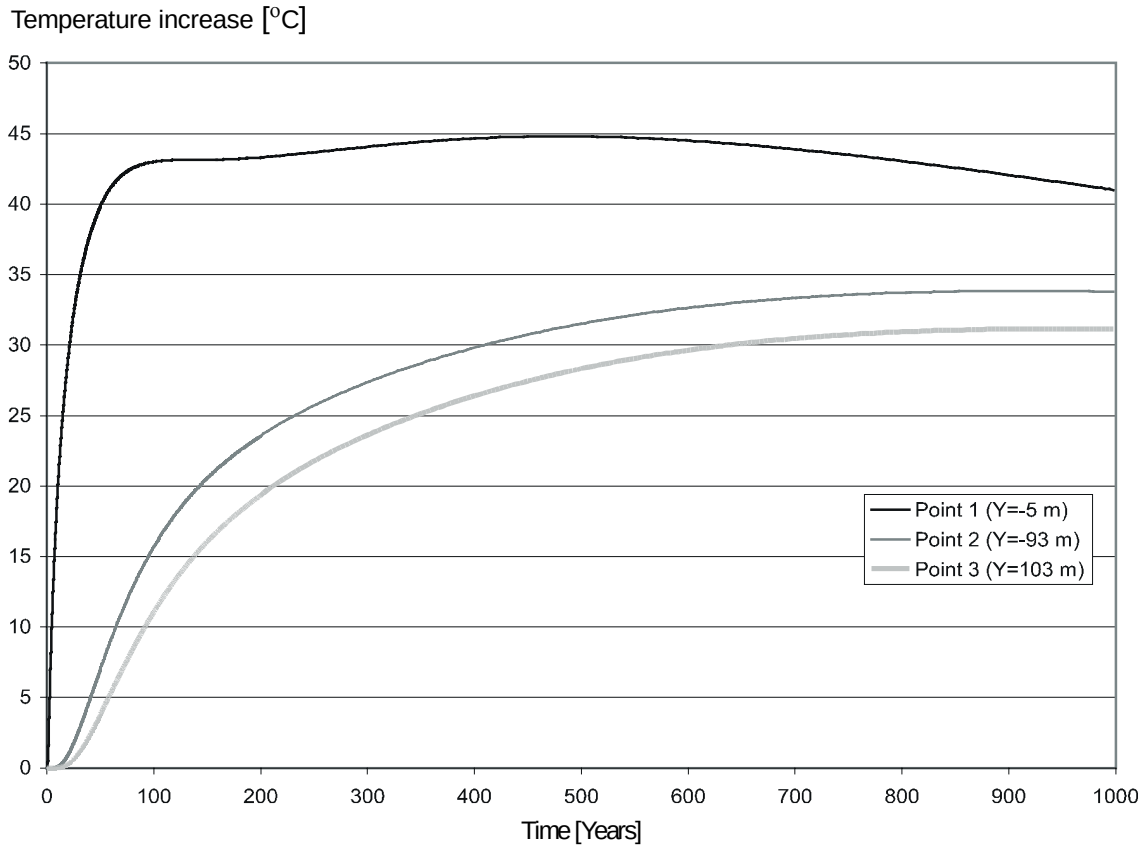

Figure 3-5. *Temperature development at three points in the model (see Figure 3-4).*

3.3.2 Stress distribution

The stress redistribution due to slip along the fracture will result in clearly increased shear stresses in the rock on both sides of the fracture ends. This distribution is prevailing already in the in-situ state (due to the ”initial” slip, see Section 3.1). To illustrate this, plots with stress tensors in the area at the upper end of the fracture in model M3 are shown in Figure 3-6, both before thermal loading and after 1000 years of deposition. The compressive stress increases from a maximum of 44 MPa to 71 MPa close to the tip. Tensile stresses also develop near the fracture end and they increase from 14 MPa to 29 MPa. It may be noted that the compressive stresses increase on the side of the fracture where the shear movement is towards the tip and tensile stresses develop on the other side of the fracture tip.

It should be remembered that the material model for the rock mass is elastic and that fracture propagation is not allowed. This explains the extent of the area having tensile stresses. In reality tensile stresses would not be expected to develop in such a large area, but tensile failure (some opening or creation of fractures in the rock mass) would instead take place. However, this discrepancy is local and it is not expected that the tensile strength of the material in the model would have a significant influence on the calculated maximum shear displacement of the fracture, which is focus of this study.

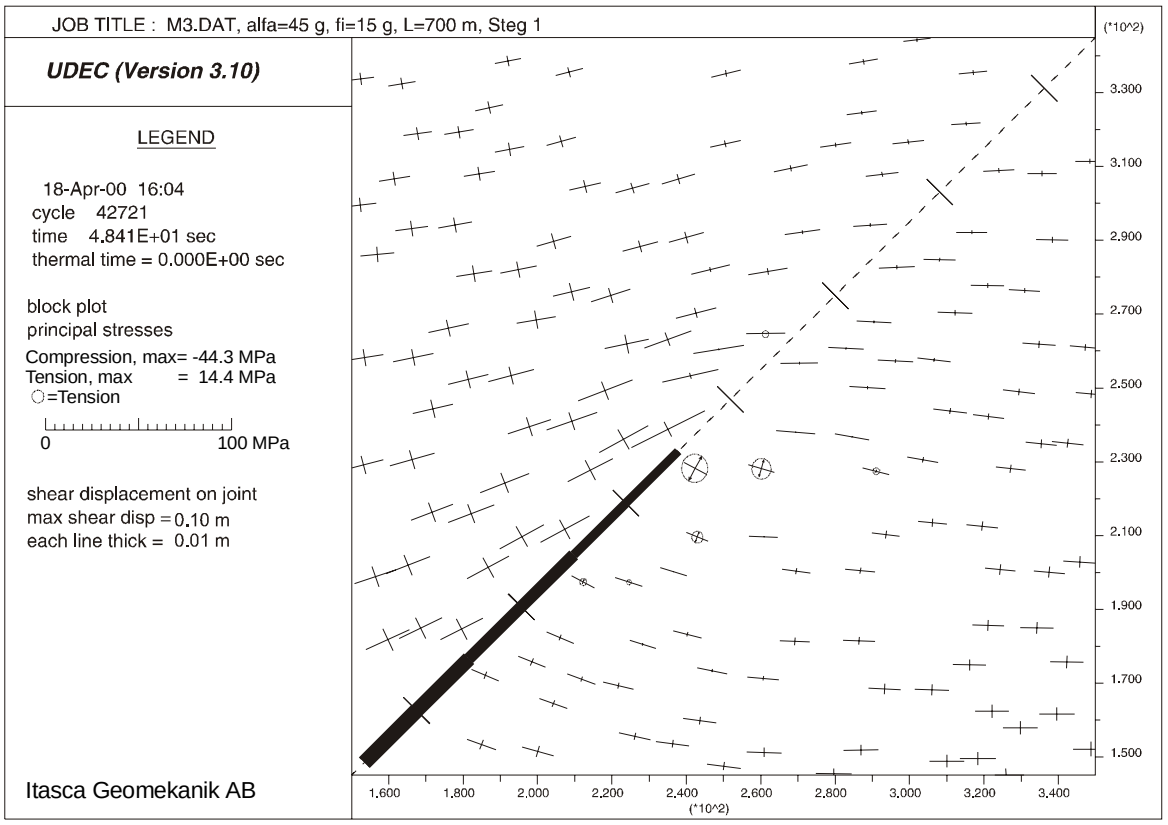

a)

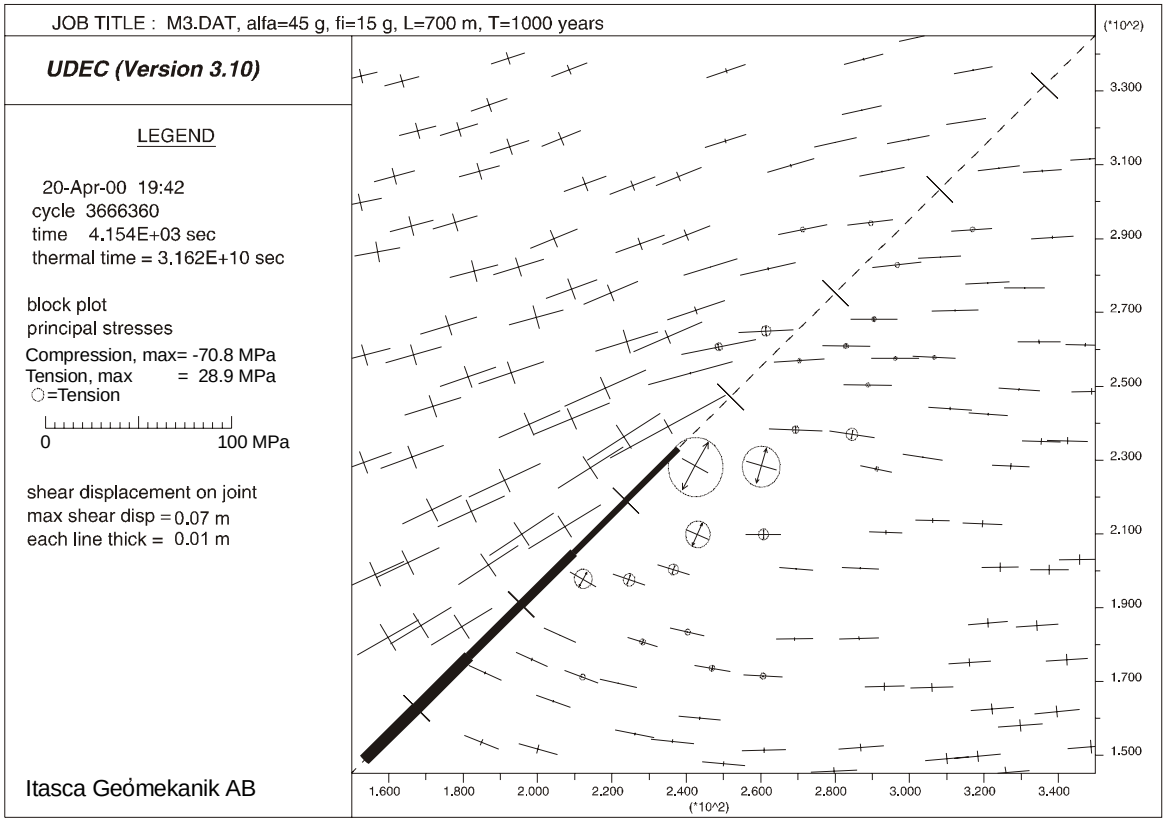

b)

Figure 3-6. *Principal stresses around upper end of the fracture a) before thermal loading and b) after 1000 years of deposition (Model M3). Shear displacements along fracture are also shown in the figures.*

3.3.3 Shear Displacements

The shear displacement of the fracture will become largest at the centre of the fracture, because the movements are constrained at the ends, and because the load is largest at the centre where the repository is located. Figure 3-7 shows the shear displacement distribution along the fracture of model M3 at 1000 years after deposition. The shear displacement will develop differently at different locations along the fracture. Figure 3-7 also shows positions in which shear displacement data were collected during the calculation. These time histories are shown in Figure 3-8. (This diagram may be compared to the temperature development diagram in Figure 3-5). The maximum shear displacement obtained at the fracture centre of each model is presented together with information about the input parameters in Table 3-1.

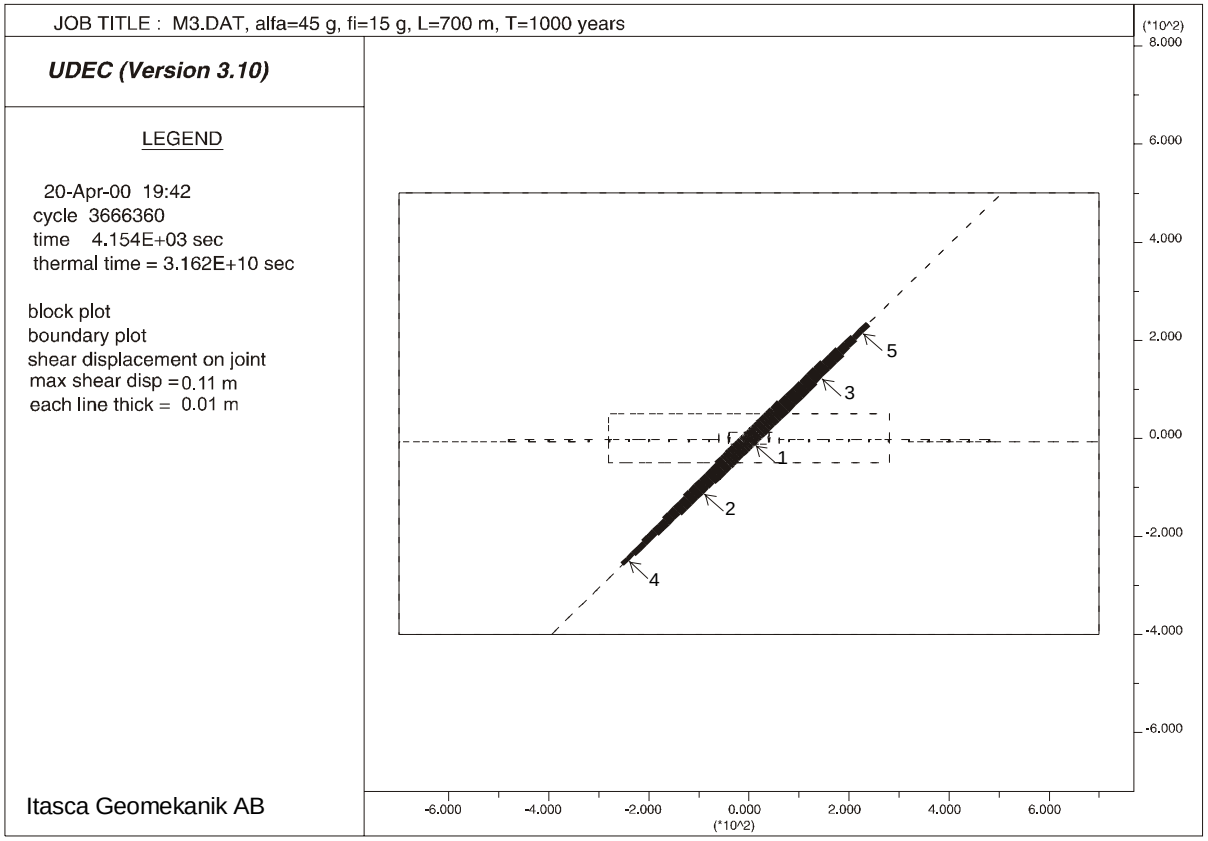

Figure 3-7. *Shear displacement distribution along fracture at 1000 years after deposition (Model M3). Locations of shear displacement histories are marked in the figure.*

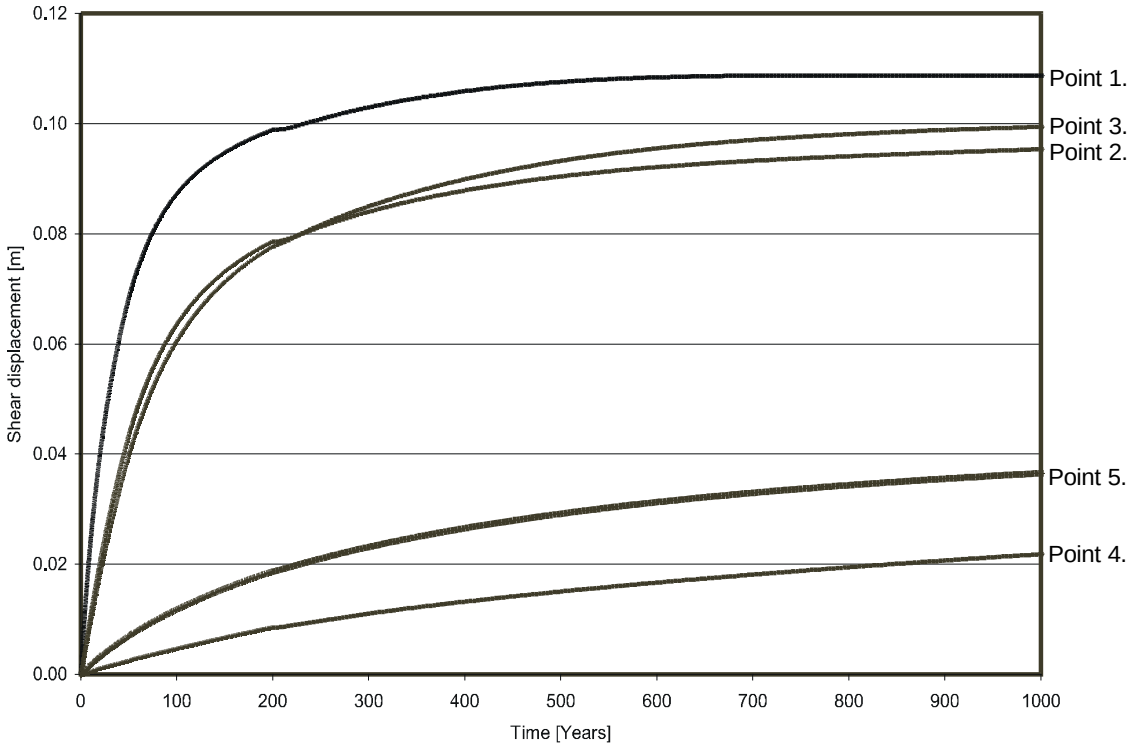

Figure 3-8. *Shear displacement development with time for five points. Point locations are shown in Figure 3-7.*

Table 3-1. Maximum shear displacement after 200 years of deposition and input parameters for each model.

Model	Dip angle [°]	Friction angle [°]	K_n [GPa/m]	K_s [GPa/m]	Length [m]	Max Shear Disp. [m]
M1	15	15	10	5	719	0.084
M2	30	15	10	5	703	0.11
M3	45	15	10	5	729	0.099
M4	45	15	100	5	729	0.099
M5	30	15	10	5	528	0.098
M6	30	15	10	5	265	0.061
M7	30	30	10	5	703	0.077
M8	30	45	10	5	703	0.002
M9	37.5	15	10	5	706	0.111
M10	30	30	10	5	528	0.069
M11	30	30	10	5	265	0.045
M12	30	5	10	5	528	0.116
M13	45	15	100	50	729	0.099
M14	15	30	10	5	719	0.038
M15	45	30	10	5	729	0.019
M16	45	30	100	5	729	0.019
M17	45	15	10	0.005	729	0.138
M18	45	15	0.1	0.005	729	0.133
M19	30	15	0.1	0.005	703	0.129
M20	30	30	0.1	0.005	703	0.134

To reduce the required modelling time it was efficient to determine the relevant time to continue calculations. The first models were run up to 1000 years and thereafter the models were calculated up to 200, 400 or 1000 years, as needed depending on the fracture dip angle. Figure 3-9 shows the maximum shear displacement of the fracture at different times in four different models. The slower response of steeply dipping fractures depends on the longer time required for the heat to reach and involve the entire fracture plane.

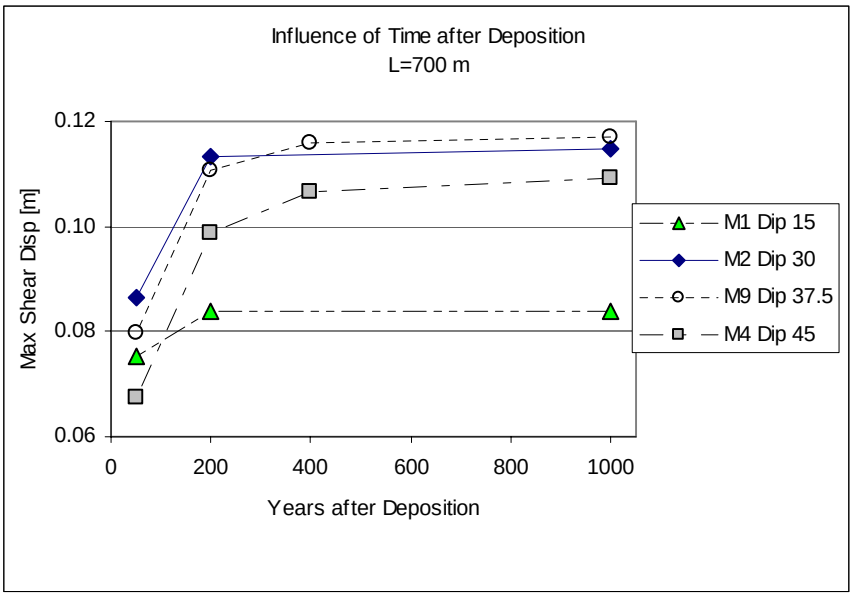

Figure 3-9. *Maximum shear displacement along fracture at different times for models with different fracture dip angle. All models have a fracture of about 700 m length and a friction angle of 15°.*

In Figure 3-10 a diagram with calculated maximum shear displacements from six models illustrates the influence of fracture length (also see the discussion about the influence of fracture length in Section 4.1). All these fractures have the same dip angle, 30°, which is the angle at which the displacement is largest. The maximum shear displacement is approximately proportional to the fracture length, which is consistent with the analytically obtained results shown in Figure 1-1.

Similarly, results are compiled in a diagram to present the influence of fracture dip, see Figure 3-11. The influence of dip becomes significant when the friction angle is fairly high. The maximum lies around a dip angle of 30°. For fractures of very low friction the dip angle has less importance. This figure can be compared with Figure 3-2, which shows shear displacements obtained in the initial equilibrium calculations. The two models which show no slip in Figure 3-2 (ϕ=30°, α=15° and 45°) are slipping for the thermal load.

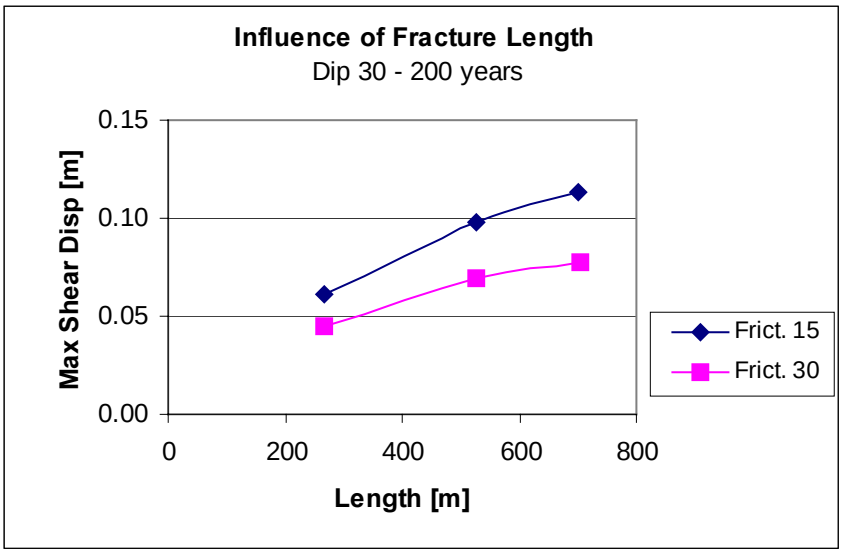

Figure 3-10. *Influence of fracture length, L, on maximum shear displacement after 200 years of deposition.*

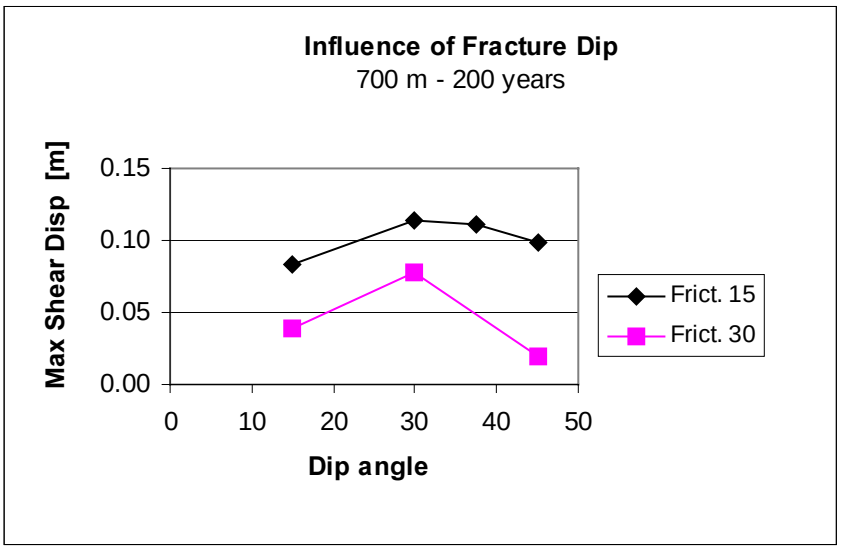

Figure 3-11. *Influence of fracture dip angle, α, on maximum shear displacement after 200 years of deposition.*

The influence of the friction angle on maximum shear displacement is further illustrated in the diagram of Figure 3-12. For the high friction angle, ϕ=45° (L=700 m and α=30°), no slip occurs for the thermal load and the shear displacement are in the elastic regime The difference in maximum shear displacement between a model with ϕ=5° and ϕ=15° is only 1.8 cm (L=500 m and α=30°).

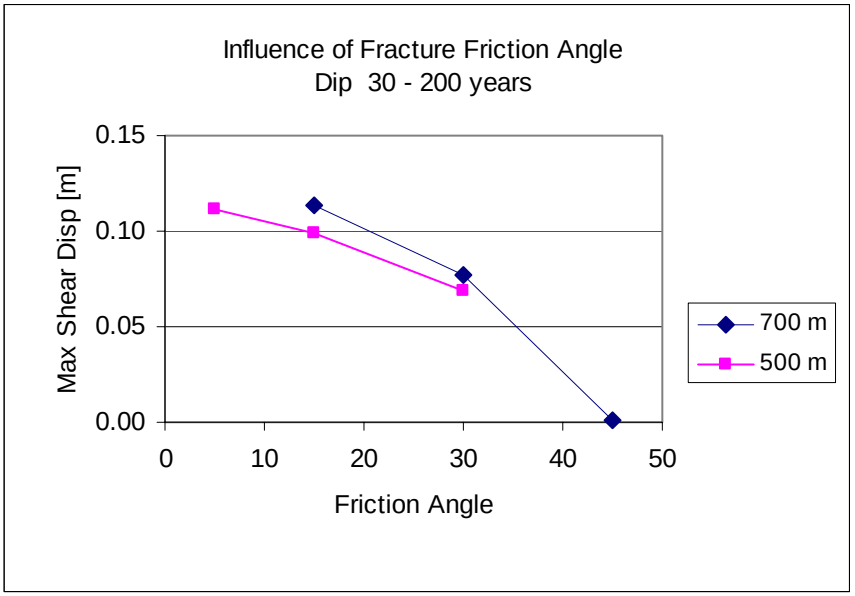

Figure 3-12. *Influence of fracture friction angle, ϕ, on maximum shear displacement after 200 years of deposition.*

Models with different shear stiffness, K_s, and different normal stiffness, K_n, were also analysed. The results of these analyses are presented in Figure 3-13 (α=45° and L=729 m) and Figure 3-14 (α=30° and L=703 m). It can be noted that if the shear stiffness is sufficiently low it will control the shear deformation, but with higher shear stiffness level the fracture will slip and the shear strength (friction angle) controls the amount of deformation obtained. The effect of the normal stiffness is expected to be less on the shear deformation since the dilation is assumed to be zero in the models.

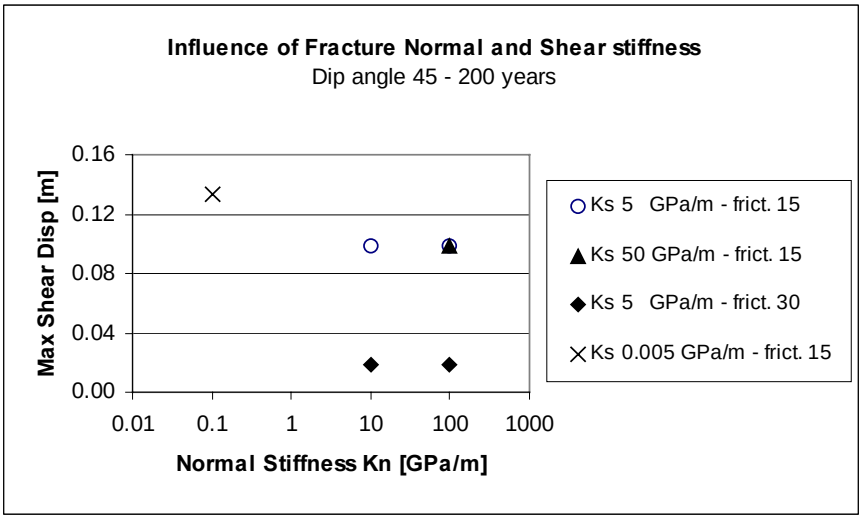

Figure 3-13. *Influence of fracture stiffness, K_n and K_s, on maximum shear displacement after 200 years of deposition for a fracture length of 729 m and a dip angle of 45°.*

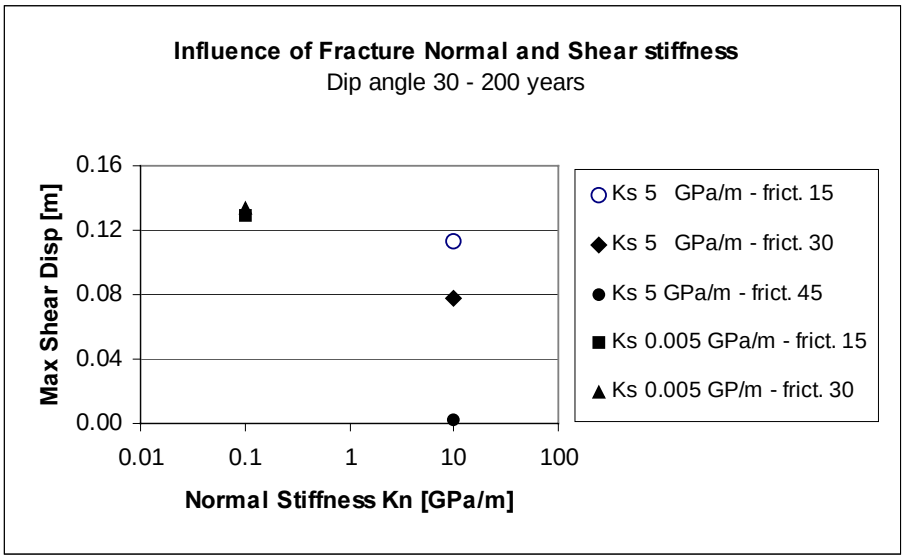

Figure 3-14*. Influence of fracture stiffness, K_n and K_s, on maximum shear displacement after 200 years of deposition for a fracture length of 703 m and a dip angle of 30°.*

4 Discussion

4.1 Fracture extension and fracture shape

The extension of a fracture, fracture zone or fault is not easy to determine. A definition of what is “start" and "end" points is needed. Also the question of what constitutes one fracture and what is two or several fractures, may not be a simple issue, in particular since the information about rock discontinuities often is limited to what can be obtained from drill holes and the ground surface.

In this study it is assumed that the fracture is one single, continuous and planar structure. This is a simpler geometry than most of structures have that will be encountered at a future repository site. But since a single fracture plane is the type of structure that would get the largest and most localized movement, and thus causing the most unfavourable loading condition around the canister, this case is the one that would be most hazardous if it was located at a deposition hole.

The fracture extension is in this two-dimensional study defined by the fracture length, L, along the dip direction of the fracture. The expected shear displacement of a fracture with the length L will depend, not only on the loading situation, but also on the extent of the fracture in other directions, i. e. on the shape of the fracture plane. A 2D-simplification of the problem, such as in the UDEC analyses reported here, will always give some overestimation of the actual shear for a certain load. In cases when the extension of the fracture is expected to be much longer in the direction parallel to the strike, the 2D-assumption would be reasonably accurate. However, if the fracture were considered to be circular, with roughly the same extension in all direction, then the 2D model would give a non-negligible overestimation of the actual shear movement.

To investigate the difference in shear displacement between these two ideal fracture shapes, a fracture with infinite extent in the strike direction (out-of-plane in UDEC models) and a circular fracture, three-dimensional analyses were performed. Using FLAC^{3D}, two models were created: one model with a fracture of circular shape and a diameter, D, and one with a fracture with the length L = D and an extension in the strike direction to the boundary of the model, See Figure 4-1a) and b) respectively. Exactly the same loading conditions and fracture strength conditions were applied for the two model cases. The dip angle of the fracture was 30° in both models. Figure 4-1 also shows isocurves of the developed shear displacement on the fracture planes. The maximum shear value occurs along the center line (or at center) of the fracture, as may be expected. For the “two-dimensional” case a) the maximum shear value is 1.4 times larger than for the circular case. (Only the relative difference between the two cases are studied and not the absolute size and displacements).

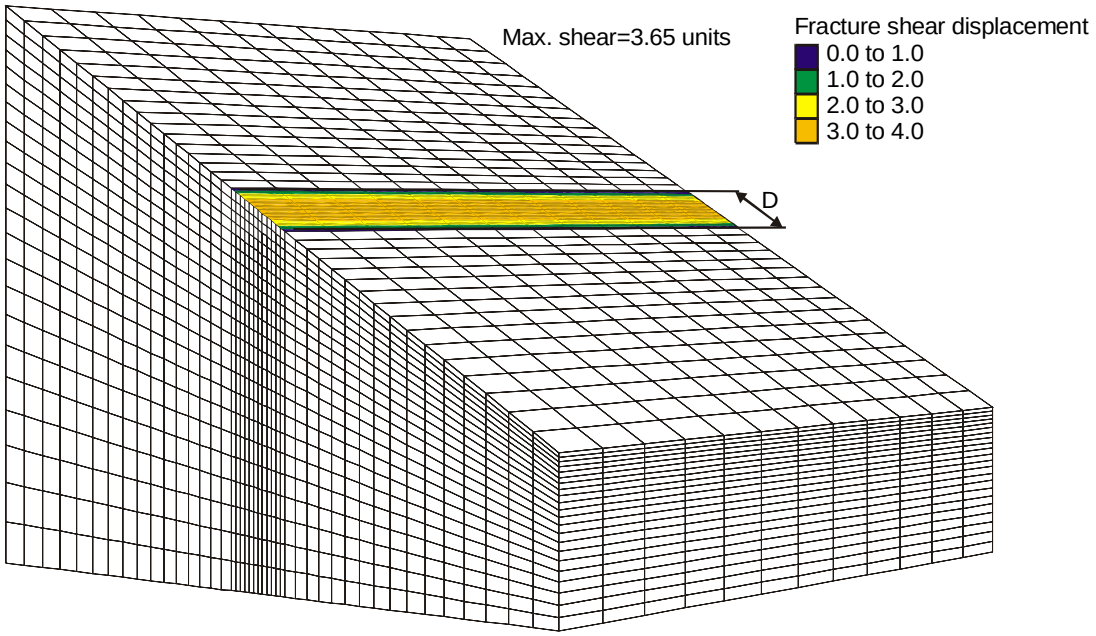

a)

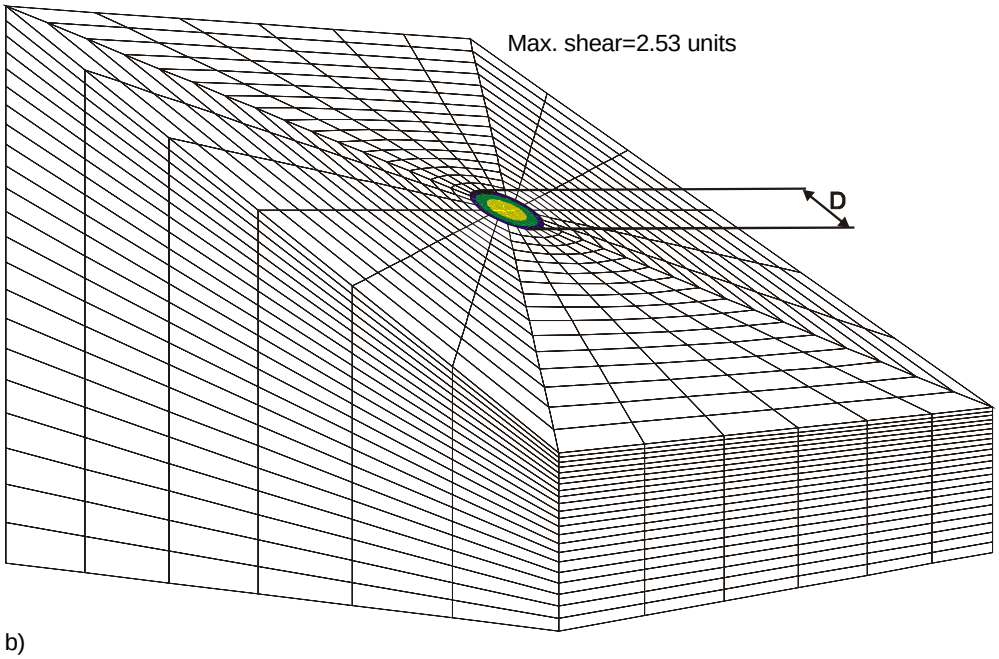

b)

Figure 4-1. *Perspective view of 3D models lower halves with shear displacements along fracture for a) "two-dimensional" fracture and b) circular fracture. (The thin lines show the finite difference grid.) The contours of the shear displacement calculated on the fracture planes are also shown in the plot, and the values of the maximum shear displacement at the center of the fractures are given. (The problem is size independent). See text.*

4.2 Fracture mechanical properties

Although it is simple to conclude that the friction properties or the shear strength of a fracture will be a main factor determining the shear displacement, it is not easy to determine these parameters for large structures with an extension of several hundreds of metres. In such cases one has to rely on the experience from previous underground construction works, in combination with findings from laboratory and field tests. In the safety assessment analyses it is thus an essential issue to consider the uncertainty or possible range of such parameters, i.e. to perform sensitivity studies.

As mentioned in Section 1.3, the approach taken here is to study the worst case, i.e. a large single fracture plane, although a much more complex geometry of a large structure is more realistic. If a fracture in the large scale is not planar, but stepped or undulating, the overall behaviour of this fracture will be dominated by the character of these steps or undulations.

Unfortunately, there is a general lack of laboratory data for weak infilled fractures. Also, laboratory test results from small samples may be difficult to interpret and apply, because of the possible scale effects and sampling biases.

As there will be a design criterion, stating which fractures should be allowed to intersect the deposition holes and which should not, there must nevertheless be established a procedure for how the strength of a discontinuity is to be estimated in the site investigation phase. This study shows that, in order that a considerable thermal-induced displacement takes place, a fracture must have a large size and a very low shear strength, where the friction angle is about 15º or lower. Studying results from discontinuity shear strength tests compiled by /Hoek and Bray, 1977/, only fractures with thick clay fillings could be expected to show such low strength. (Where fillings are thicker than the asperities of the fracture surfaces, the shear strength becomes controlled by the properties of the filling material rather than the rock properties). This implies that focus of the site investigation, with respect to the shear displacement safety criterion, should be to locate and characterize clay-filled fractures that may intersect the planned repository area.

The model analyses performed with different shear stiffness did result in slightly different shear displacement for the stiffness range investigated. When the shear stiffness is high the friction will control the total shear deformation. This may be seen when comparing the model M2 with M7 or the model M1 with M14 (See Table 3-1). On the other hand, if the shear stiffness is very low the total shear deformation will be controlled by the stiffness, irrespective of the friction. This is seen when comparing the model M19 with M20. They both resulted in similar shear displacement although they have different friction angle. The fracture normal stiffness does not influence the results when, as in this case, there is no dilation assumed for the fracture.

4.3 Rock mass properties

The rock mass surrounding the single fracture has in this study been simulated as a homogeneous, isotropic and elastic material. This means that the modulus of elasticity, i.e. Young's modulus, applied for this material should represent the overall deformation properties of the rock mass, consisting in reality of both intact rock blocks and fractures of different order. In this study a Young's modulus of 40 GPa was selected as it was

considered to be a reasonable value, corresponding to results from a back-analysis from the excavation work in the Oskarshamn area. According to laboratory tests of intact rock in the area (performed on core samples during the construction of the Äspö HRL) the mean Young's modulus for four rock types tested was in the range 73–78 GPa /Stille and Olsson, 1996/.

However, it should be mentioned that the value of the Young's modulus of the rock mass is scale dependent and may vary from site to site. The reason for large variations in rock mass deformation properties can lie both in the properties of the intact rock type and in the properties of the fractures (faults, joints, fracture zones) in the area. For this particular study the Young's modulus is, however, not an important factor (see below).

In general, thermo-mechanical effects will depend both on the thermal expansion coefficient and the elastic modulus of the material, since they determine the deformation and the stress change that result from the thermal expansion. In addition to the twenty models presented earlier in this report, two models were analysed concerning the influence of the Young's modulus and the thermal expansion coefficient. Results from these models are discussed below.

A comparison was made between a UDEC model having 50 GPa Young's modulus instead of 40 GPa (all other input parameters were the same as for model M2, see Table 2-1). This comparison showed that the stresses at the fracture ends increase with the higher modulus, but that the maximum shear displacement is almost the same. The reason to this is that in the cases where the fracture is at slip failure, the total displacement is controlled by the total "available" expansion determined by the expansion coefficient, which was in this case held constant.

A comparison was also made between two models with different thermal expansion coefficients, 8.5e-6 1/°C (model M2) and 9.5e-6 respectively. This comparison showed that a 12% increase in thermal expansion coefficient resulted in a 16% increase in shear displacement (13.1 cm instead of 11.3 cm) at the centre of the fracture. The uncertainty in the thermal expansion coefficient value is regarded as fairly low, since this parameter may be determined in laboratory.. The contribution to the uncertainty in shear displacement due to the thermal expansion coefficient should thus be minor.

The thermal conductivity determines the time for the heat to spread in the surrounding rock. A change in this parameter in a model would thus result in a change in the temperature development with time in an arbitrary point, i.e. the temperature distribution at a certain period of time after deposition would be different. Lower thermal conductivity results in higher maximum temperatures around the repository and accordingly a larger shear displacement due to the thermal expansion would be expected. The thermal conductivity can be determined on rock samples in the laboratory. According to /Sundberg, 1988/ the average thermal conductivity for granitic and gneissic rocks lies around 3.5 W/mº C. The conductivity decreases slightly with temperature. In this study the fairly conservative value 3.0 W/mº C was used.

5 Conclusions and recommendations

Two-dimensional analyses using the UDEC code have been performed. The UDEC model represents a vertical cross section of the repository with a hypothetical planar fracture intersecting a deposition hole at the repository centre. Initial stresses and rock conditions were held constant and influence of different fracture geometries and properties were studied.

The simulated fracture shear displacements occur due to the thermal expansion of the rock surrounding the heat generating canisters. The initial heat release per unit repository area was assumed to be 8W/m². The thermo-mechanical analysis shows that the maximum shear is reached after about 200–400 years, earlier the more parallel to the repository horizon the fracture plane is.

The largest displacement occurs at the fracture centre, which is in this case located at the repository level, and the magnitude of shear depends on the different assumptions made for the twenty different models analysed. Among the analysed cases, the largest shear values, about 13 cm, was calculated for the cases with about 700 m long fractures with a shear stiffness of 0.005 GPa/m. Also, for large fractures with a higher shear stiffness of 5 GPa/m, but with a low friction angle (15°), the shear displacement reaches similar magnitudes, about 10 cm. As an example of a smaller shear, 4.5 cm displacement was obtained for the case with a fracture of 265 m length, 30° fracture friction and 30° dip angle (model M11). A case with a very high friction angle (45°), and 5 GPa/m shear stiffness, resulted in a maximum shear of only 0.2 cm (model M8).

Fracture extension is the main factor in the estimation of shear displacements. For example, for a fracture with 30° dip angle and about 500 m length in the dip direction, a change of the length by 100 metres, would correspond to maximum 3 cm change in the expected shear displacement in a two-dimensional case.

For a fracture of given extension, fracture friction angle and fracture shear stiffness are important parameters for the estimation of expected shear displacement. A 10° change in friction angle would imply a change in estimated shear displacement of 3–5 cm, for a fracture with 30° friction. If the fracture shear stiffness is sufficiently low shear displacements are will not depend on friction. The development of a procedure for the estimation (or classification) of fracture friction and fracture shear stiffness, are therefore identified as important tasks for the site investigation phase. A very low friction value is expected only for fractures (or faults) with substantial clay filling material.

Also, the estimated shear displacement will depend on the assumed shape of the fracture. In the two-dimensional UDEC analyses, the fracture extension is represented by its length, L, in the dip direction and an infinite extension in the out-of-plane direction. If instead the shape of the fracture were assumed to be circular, with the diameter L, the expected shear would be smaller. Results from additional three-dimensional analyses performed (using FLAC^{3D}) show that a fracture, with length L in the dip direction and infinite extension in the strike direction, gives 1.4 times larger maximum shear displacement compared to a circular fracture with a diameter L. Thus,

if the calculated shear value, for the case giving the largest shear displacement (L= 729 m, ϕ =15° and α = 45°), is corrected for an assumed circular fracture shape (i.e. by dividing the value with 1.4) the maximum shear displacement instead becomes 9.9 cm.

For fractures with a friction angle around 30°, the dip angle is an important factor in terms of fracture shear displacement changes. A fracture with a dip angle of 30° instead of 45° results in approximately four times larger maximum shear displacement. This effect is, however, smaller for fractures with lower friction angles.

Factors other than fracture friction angle, shear stiffness, extension and dip angle have less influence on the estimation of maximum shear displacement.

The current safety limit for allowed fracture shear displacements across a deposition hole is ten centimetres. This study shows that it takes fractures of very large extension, several hundred meters, to produce thermally induced shear displacements of this magnitude. If the central parts of such fractures intersect the repository, they will be identified early in the layout and construction process.

With regard to the 0.1 m displacement criterion and with regard to the thermal load, the results of this study suggest the following approximate mechanical layout restriction for a future KBS-3 repository: Central parts of fractures dipping in the range of 30–45° with a minimum length of 700 metres in the dip direction, and a friction angle smaller than about 15°, or shear stiffness on the order of 0.005 GPa/m or less should not be allowed to intersect any deposition holes. This recommendation is only valid for the over all conditions assumed in this study. A significantly different initial stress state or change in thermal loading could lead to different layout restrictions.

6 Acknowledgements

This study was funded by the Swedish Nuclear Waste Management Company (SKB). The valuable contribution to the work from the members of the project reference group, Rolf Christiansson (SKB), Harald Hökmark (Clay Technology) and Anders Fredriksson (Golder Grundteknik), is acknowledged. We also thank Lars Rosengren (Rosengren Bergkonsult) for his review of the report.

References

Hakami E, Olofsson S-O, Hakami H, Israelsson J, 1998. Global Thermo-Mechanical Effects From a KBS-3 Type Repository Summary Report.
SKB TR-98-01, Svensk Kärnbränslehantering AB

Hoek E, Bray J W, 1977. Rock Slope Engineering.
The Institution of Mining and Metallurgy, London. ISBN 0 900488 36 0

Itasca, 2000. UDEC Users Manual, Vol I–III, Itasca Consulting Group Inc, Minneapolis.

Leijon B, 1993. Mechanical properties of fracture zones.
SKB TR-93-19, Svensk Kärnbränslehantering AB

Pollard, D D, Segall P, 1987. Theoretical displacements and stresses near fractures in rock: with application to faults, joints, veins, dikes, and solution surfaces.
Fracture Mechanics of Rock, Academic Press Inc, London.

Rehn I, Gustafson G, Stanfors R, Wikberg P, 1997. ÄSPÖ HRL – Geoscientific evaluation 1997/5. Models based on site characterization.
SKB TR-97-06, Svensk Kärnbränslehantering AB

SKB, 1998. RD&D-Programme 98 – Treatment and final disposal of nuclear waste.
Svensk Kärnbränslehantering AB

SKB, 1999. SR 97 – Processes in the repository evolution.
SKB TR-99-07, Svensk Kärnbränslehantering AB

Stille H, Olsson P, 1996. Summary of rock mechanical experiences from the construction of Äspö Hard Rock Laboratory.
SKB PR HRL-96-07, Svensk Kärnbränslehantering AB

Sundberg J, 1988. Thermal properties of soils and rocks.
Doctoral Thesis, Dept of Geology, Chalmers University of Technology, Gothenburg

Thunvik R, Braester C, 1991. Heat Propagation From a Radioactive Waste Repository Complementary Calculations for the SKB 91 Reference Canister
SKB TR-91-17, Svensk Kärnbränslehantering AB